Journal of Animal & Plant Sciences, 36(1): 2026, Page: 58-68
ISSN (print): 1018-7081; ISSN (online): 2309-8694
https://doi.org/10.36899/JAPS.2026.1.0005

SYNTHESIS AND CHARACTERIZATION OF HOLLOW SILICA NANOPARTICLES WITH PALLADIUM: ASSESSING GERMINATION TRAITS IN *CAMELINA SATIVA* L.

M. Ghorbani[1], Z. Chaghakaboodi[2] and D. Kahrizi[3*]

[1]Department of Nanobiotechnology, Faculty of Strategic Sciences and Technologies, Razi University, Kermanshah, Iran. E-mail: masoomeh.ghorbani0072@gmail.com
[2]Department of Production Engineering and Plant Genetics, Faculty of Science and Agricultural Engineering, Razi University, Kermanshah, Iran. E-mail: z.chaghakaboodi@razi.ac.ir
[3]Department of Biotechnology, Faculty of Agriculture, Tarbiat Modares University, Tehran, Iran. E-mail: dkahrizi@modares.ac.ir
[*]Corresponding author's: E-mail: dkahrizi@modares.ac.ir

ABSTRACT

Given the necessity of promoting and expanding the cultivation of oilseed plants, including Camelina, and the importance of assessing the effects of nanoparticles on the environment and agriculture, an experiment was conducted to evaluate the impact of different concentrations of synthesized palladium nanoparticles (0, 50, 100, and 200 mg/L) on certain germination indices of the Soheil cultivar of Camelina. These indices included germination percentage, root length, shoot length, and the root-to-shoot length ratio. In this study, hollow silica nanoparticles loaded with palladium metal were synthesized on hollow mesoporous silica functionalized with an organic ligand (HMSNs~Pyra/Pd). The characteristics of the palladium nanoparticles (PdNPs) were analyzed employing Fourier-transform infrared spectroscopy (FTIR), scanning electron microscopy (SEM), transmission electron microscopy (TEM), and energy-dispersive X-ray spectroscopy (EDX). The study was designed as a completely randomized experiment with three replications under in vitro conditions. The morphology results of the nanoparticles, analyzed using TEM, indicated an average size of 30–50 nm for HMSNs~Pyra/Pd nanoparticles and approximately 5–8 nm for palladium nanoparticles. The SEM images showed nanoparticles with an average size of around 25–35 nm, which was consistent with the TEM findings. FT-IR analysis also revealed that the signal corresponding to the asymmetric stretching vibration of the Si-O-Si bond appeared at approximately 1095 cm^{-1}. The bonds at 807 cm^{-1} and 1468 cm^{-1} corresponded to the symmetric stretching vibration of Si-O, confirming the presence of the SiO_2 layer. The elemental analysis of the synthesized nanoparticles using EDX confirmed the presence of C, N, Si, O, and Pd in the structure of HMSNs~Pyra/Pd nanoparticles. This confirms the successful functionalization of the hollow silica nanoparticles using this technique. The results also indicated that different concentrations of palladium nanoparticles had a significantly negative effect on all the studied germination traits of the Camelina plant. The highest germination percentage (95%) was observed in the control group, while the lowest (67.11%) was recorded at the 200 mg/L palladium nanoparticle concentration.

Keywords: Co-precipitation method, Germination Percentage, Hollow Silica Nanoparticles, Pyrazolone, Sol-gel method.

Published first online November 13, 2025 Published final January 20, 2026

INTRODUCTION

In recent decades, global interest in sustainable agriculture and green technologies has driven research into novel materials and methods to improve crop productivity and resilience (Prasad *et al*., 2016). Among these, nanotechnology has emerged as a transformative tool in plant sciences, offering unique opportunities to manipulate biological systems at the nanoscale. Nanoparticles (NPs), particularly those smaller than 100 nanometers, possess distinctive physical, chemical, and biological properties that can influence plant growth, development, and stress responses (Sayedena *et al*., 2019). The production of nanoparticles and their applications in various aspects of plant sciences are increasing. Despite the growing production of these particles, there are limited studies on the effects of different nanomaterials on plant biology. The term nanotechnology, derived from the Greek suffix "nano," means small. More specifically, nano refers to one billionth of a meter. The term nanotechnology is generally used for materials that have sizes ranging from one to one hundred nanometers**.** These materials, due to

their small size, should exhibit distinct properties compared to larger materials. These differences include physical forces**,** chemical reactivity, electrical conductivity**,** magnetic effects**,** and optical properties (Findik. 2021). According to plant biology specialists**,** only nanoparticles with a diameter of less than 20 nanometers are capable of passing through the cell wall**,** as the average diameter of pores in plant cell walls ranges from 5 to 20 nanometers. Therefore, nanoparticles within this size range can enter the cell interior and intracellular membranes. The study of nanoparticles and their effects on plant growth is quite complex, as there are varying reports on the effects of nanoparticles on different plants. However, the main concern has been the toxicity of nanoparticles on plants and ecosystems, which is an area of ongoing research (Sayedena *et al*., 2019). Today, with the expansion of nanotechnology and the production of nanoparticles in various fields, along with their increasing application in industry, pharmaceuticals, and energy production, concerns have arisen regarding the potential environmental and health risks posed by these nanoparticles. These risks have attracted the attention of many environmental experts. Studies on the fate of nanoparticles in the environment are limited, and these particles may eventually enter the food chain, potentially affecting humans. Plants are the most important component of the ecological system through which nanoparticles can be transferred to other organisms (Vijay *et al*., 2025). Plants may absorb these materials via various pathways, such as contaminated soil and water (Kelij and Kazemian Ruhi, 2018).

The oilseed plant Camelina (*Camelina sativa* L.) is an oil-bearing crop belonging to the Brassicaceae family, with multiple properties and applications. In nutrition and health, its oil is rich in omega-3 fatty acids, which help prevent cancer and obesity. In industry, it is used for biofuel production, resin and wax manufacturing, as well as in the production of cosmetic, hygiene, and pharmaceutical products (Ghorbani *et al*., 2020).

Germination is the first and most critical stage in a plant's life cycle, playing a key role in the survival and preservation of plant species. In modern agriculture, fast, robust, and successful seed germination is crucial for ensuring optimal plant growth and high crop yields. As a result, any factor that affects germination will inevitably influence the plant's future development (Khan *et al*., 2022). The impact of Ag NPs on the germination rates of rice and pea seeds, alongside the influence of fourteen distinct nanomaterials on plant physiological processes and functional differentiation in 356 maize specimens, was investigated across a range of nanoparticle sizes. Ag NPs with diameters of 77.5, 111.7, 68.6, and 98.9 nm achieved a maximum germination rate of 100% in peanut seeds. Conversely, Ag NPs measuring 77.5 and 111.7 nm were associated with reduced germination rates in maize and rice relative to the control group (Prasad *et al*., 2016). Research has been conducted on the positive and negative effects of nanoparticles on higher plants. For example, the combination of SiO_2 and TiO_2 nanoparticles has been reported to accelerate germination rates in crops like soybeans (Gohar *et al*., 2024). According to the statements of Skiba *et al*., (2024), The positive effects of TiO_2 are concentration-dependent, with specific optimal levels yielding the best results in terms of growth and metabolic enhancement. Titanium dioxide nanoparticles have been shown to influence various physiological parameters in *Rosmarinus officinalis*, including cell growth, cell division, cell size, callus induction, and the levels of phytohormones such as gibberellins and cytokinins, with treated plants exhibiting significant increases in these factors (Golami *et al*., 2020). In a separate investigation, the effects of zirconium dioxide (ZrO_2), silicon dioxide (SiO_2), aluminum oxide (Al_2O_3), and titanium dioxide (TiO_2) nanoparticles on maize seed germination were evaluated. The study reported a reduction in germination percentage following treatment with Al_2O_3 and TiO_2 nanoparticles, whereas SiO_2 nanoparticles consistently enhanced germination across all growth conditions. Furthermore, seed uptake of these metal nanoparticles was highest for SiO_2, followed sequentially by TiO_2, Al_2O_3, and ZrO_2 (Karunakaran *et al*., 2016). Meanwhile, AgNPs have been shown to decrease the mitotic index in onion root tips, indicating reduced cell division, except at very low concentrations (5 mg/L), where an increase was observed (Abd-elhamed, 2017). Heydari *et al*., (2015) also conducted a study on the effect of silicon nanoparticles on germination and seedling growth of various native and improved wheat cultivars under laboratory conditions. Their results showed that silicon nanoparticles increased vigor and led to more uniform seedling emergence in wheat plants. Furthermore, a study investigating the impact of AgNPs on the growth of the L-883 variety of *Allium cepa* L. utilized AgNPs with a particle size of 100 nm at four distinct concentrations (25, 50, 75, and 100 ppm). The results indicated that the 25 ppm concentration of AgNPs yielded the highest seed germination percentage compared to the other tested concentrations. Conversely, higher concentrations exhibited detrimental effects on both seed germination and seedling development, with toxicity levels demonstrating a strong positive correlation with the concentration of the nanoparticle suspensions (Patidar *et al*., 2024). Given the unique physiological characteristics of Camelina and the growing application of nanomaterials in modern agriculture, this study hypothesizes that hollow silica nanoparticles loaded with palladium (Pd-HSNPs) could influence the germination process of Camelina seeds. The objective of this research was to synthesize Pd-HSNPs and evaluate their effects on seed germination indices—including germination rate, percentage, and seedling vigor—under in vitro

conditions. By examining the potential stimulatory or inhibitory effects of Pd-HSNPs, this study aims to provide foundational insights into the safe and effective use of engineered nanoparticles in oilseed crop development.

MATERIALS AND METHODS

Characterization of Synthesized Nanoparticles: This research was conducted in the tissue culture laboratory of the Faculty of Agriculture and Natural Resources at Razi University in 2024. All chemicals used in this study, including tetraethyl orthosilicate (TEOS, purity = 98%), cetyltrimethylammonium bromide (CTAB, purity ≥98%), 3-chloropropyltrimethoxysilane (CPTES, purity ≥97%), palladium acetate with purity ≥99.9%, and sodium borohydride with purity ≥99%, were sourced from Fluka, Merck, and Sigma-Aldrich and were utilized as received, without additional purification, unless specified otherwise. The morphology and elemental composition of the synthesized nanoparticles were analyzed using Transmission Electron Microscopy (TEM) with a FEI Tecnai G2 F20 instrument. Additionally, Scanning Electron Microscopy (SEM) images were acquired employing a Quanta 450 SEM system (FEI, USA) equipped with an Energy Dispersive X-ray Spectroscopy (EDX) analyzer (EDAX) at an accelerating voltage of 20 kV. TEM analysis was performed operated at 100 kV electron beam accelerating voltage, and for SEM analysis, lyophilized nanoparticles were mounted on aluminum stubs using double-sided carbon tape and sputter-coated with gold to enhance conductivity. The molecular structures and compositions of the materials were examined utilizing Fourier-transform infrared spectroscopy (FTIR) with a Bruker Tensor 27 instrument. Analyses were conducted on powdered samples across the spectral range of 400 to 4000 cm^{-1}, employing a resolution of 4 cm^{-1} and accumulating 32 scans per sample.

Synthesis of Palladium Nanoparticles: Palladium nanoparticles were synthesized on hollow mesoporous silica functionalized with an organic ligand according to the method described by Ghorbani *et al*., 2021.

Synthesis of silica-coated magnetite NPs (Fe_3O_4@CTAB/SiO_2 NPs): Magnetite (Fe_3O_4) nanoparticles were synthesized utilizing a co-precipitation technique as previously reported by Ghorbani *et al*. (2025). Briefly, 2.7 g of $FeCl_3 \cdot 6H_2O$ and 1.0 g of $FeCl_2 \cdot 4H_2O$ were dissolved in 130 mL of deionized water under a nitrogen atmosphere with vigorous stirring. Subsequently, 25% ammonia solution was added until the pH reached 11, and the reaction mixture was maintained under stirring at 60 °C for an additional hour. The resulting magnetite precipitate was isolated magnetically, washed thoroughly, and air-dried.

Following this, Fe_3O_4@CTAB/SiO_2 nanoparticles were fabricated by coating the Fe_3O_4 cores with a mesoporous silica shell via a sol-gel process, as described by Ghorbani *et al*. (2024). Specifically, 0.1 g of Fe_3O_4 nanoparticles and 0.60 g of cetyltrimethylammonium bromide (CTAB) were dispersed in a solvent mixture comprising 60 mL ethanol and 100 mL water through ultrasonic treatment for 30 minutes. Subsequently, 6.0 mL of 25% ammonia solution was introduced, followed by the gradual addition of 3.0 mL tetraethyl orthosilicate (TEOS) dissolved in 20 mL ethanol under continuous stirring. The reaction mixture was then allowed to proceed at 30 °C for 24 hours. The final Fe_3O_4@CTAB/SiO_2 nanoparticles were recovered via magnetic separation, washed with water and ethanol, and dried under vacuum conditions.

Preparation of hollow mesoporous silica NPs (HMSNs): Fe_3O_4@CTAB/SiO_2 NPs were dispersed in acidic ethanol (37% HCl) and subsequently heated to 80 °C. The resulting suspension was continuously stirred overnight to ensure the thorough removal of the templates.

Preparation of modified HMSNs (HMSNs~Cl): In summary, 0.2 g of synthesized HMSNs were dispersed in 10 mL of anhydrous toluene and subjected to ultrasonic treatment. Subsequently, 0.6 mL of CPTES was introduced into the suspension. The reaction mixture was then refluxed with continuous stirring at 110 °C for 24 hours. Upon completion, the mixture was allowed to cool, followed by centrifugation and sequential washing twice with ethanol and distilled water to remove any residual unreacted CPTES. The purified HMSNs~Cl were finally dried under vacuum at 60 °C for 24 hours. Thereafter, the organic ligand containing a pyrazolone functional group was synthesized following the procedure previously described by Ghorbani *et al*. (2021).

Preparation of HMSNs~Pyra/Pd NPs: An aqueous solution of $Pd(OAc)_2$ (0.134 g in 30 mL water) was prepared and subsequently combined with 0.3 g of HMSNs~Pyra. The resulting mixture was stirred for 30 minutes, producing a brown suspension. Thereafter, a $NaBH_4$ solution (0.11 g in 10 mL ethanol) was added. The reaction mixture was maintained under stirring at 60 °C for 6 hours. Following completion, the product was isolated by centrifugation, washed twice with ethanol, and dried overnight at 70 °C, affording dark gray HMSNs~Pyra/Pd.

Experimental Treatments: A factorial experiment was conducted using a completely randomized design (CRD) with three replications to examine the impact of palladium nanoparticles on the germination characteristics of the *Camelina sativa* cultivar Soheil. For

seed germination, 20 surface-sterilized seeds of *Camelina sativa* cultivar Soheil were placed in each Petri dish on sterile filter paper. Palladium nanoparticle solutions at concentrations of 0, 50, 100, and 200 mg/L were used as treatments. In the control treatment (0), distilled water was used. The seeds were placed in each Petri dish containing 12 mL of the different nanoparticle solutions and incubated at 25°C for 10 days, with 20 seeds per dish. The Petri dishes were subsequently placed in a germinator programmed to maintain a photoperiod consisting of 16 hours of light followed by 8 hours of darkness in an alternating cycle. A ruler was also used to measure the traits of Radicle Length and Shoot Length. The traits measured in germination include the following:

1- Germination Percentage (%): The formula for germination percentage is as follows (Larsen and Andreasen, 2004):

Germination Percentage (%) = (Number of seeds germinated /Total number of seeds tested) ×100

2-Radicle Length (cm): The length of the part of the seedling that grows downward (root).

3-Shoot Length (cm): The length of the part of the seedling that grows upward (stem).

4-Root-to-Shoot Ratio (cm): The comparison of the length of the root to the length of the shoot, indicating the plant's development balance.

Statistical analysis: We applied one-way ANOVA using aov function in stats package 4.3.1 in R, followed by Duncan multiple range test ($p < 0.05$) for mean comparison via Duncan. Test function in agricolae package 1.3.7 in R. Heatmap visualization was conducted using the ClustVis web-tool (Metsalu and Vilo, 2015). To gain a deeper understanding of the different traits, pairwise correlation analysis was calculated using R software.

RESULTS AND DISCUSSION

Fourier Transform Infrared (FT-IR) Spectroscopy: Fourier-transform infrared (FT-IR) spectroscopy was performed to verify the presence of functional groups, confirm the successful functionalization of the nanoparticles, and ensure the removal of surfactant (CTAB) and Fe_3O_4 components used during synthesis. The FT-IR spectrum of the HMSNs~Pyra/Pd nanoparticles is shown in Figure 1, revealing distinct vibrational bands characteristic of the functional groups present in the structure. A strong and broad absorption band observed around 1095 cm^{-1} corresponds to the asymmetric stretching vibrations of Si–O–Si bonds, confirming the formation of a siloxane (Si–O–Si) network, which is typical of silica-based nanomaterials. In addition, peaks at approximately 1807 cm^{-1} and 1468 cm^{-1} are assigned to the symmetric stretching modes of Si–O, further confirming the successful synthesis of a silica (SiO_2) shell. The presence of organic moieties was confirmed by several key vibrational peaks. The signals observed at 1656 cm^{-1} and 1552 cm^{-1} correspond to C=C stretching vibrations of aromatic rings, while a broad band at 3389 cm^{-1} is attributed to the O–H stretching vibration, indicating the presence of hydroxyl groups. These signals confirm the successful grafting of the organic ligand 4,4′-((4-hydroxyphenyl) methylene) bis (3-methyl-1H-pyrazol-5-ol) onto the surface of the hollow silica nanoparticles. In addition, weak signals related to C–H stretching vibrations and C–Cl stretching from CPTES (3-chloropropyltrimethoxysilane) appear in the fingerprint region, indicating that CPTES was used effectively for surface modification prior to ligand attachment. Importantly, no residual peaks were detected in the region corresponding to CTAB (cetyltrimethylammonium bromide) or Fe–O bonds, typically appearing around 580–650 cm^{-1}, suggesting that both the surfactant template and Fe_3O_4 magnetic cores were successfully removed during purification, consistent with earlier findings (Soleimani *et al*., 2012). These spectral results confirm the successful synthesis, functionalization, and purification of the HMSNs~Pyra/Pd nanomaterials, with well-defined inorganic (SiO_2) and organic (pyrazole ligand) components.

Morphology of Nanoparticles: The morphology of the nanoparticles was observed using Transmission Electron Microscopy (TEM). In Fig 2-A, the TEM image shows an average size range of 30-50 nm for the HMSNs~Pyra/Pd nanoparticles, with palladium nanoparticles having an approximate size of 5-8 nm. This confirms the successful synthesis of palladium nanoparticles on the surface of hollow silica nanoparticles. Fig 2-B displays the Scanning Electron Microscopy (SEM) image of the nanoparticles, showing a spherical morphology with an average size of approximately 25-35 nm, which is consistent with the size observed in the TEM image.

Energy Dispersive X-ray Spectroscopy (EDX) Analysis: The elemental composition of the synthesized nanoparticles was analyzed using Energy Dispersive X-ray Spectroscopy (EDX). As shown in Figure 3, the EDX spectrum confirmed the presence of carbon (C), nitrogen (N), silicon (Si), oxygen (O), and palladium (Pd) in the structure of the HMSNs~Pyra/Pd (Hollow Mesoporous Silica Nanoparticles functionalized with Pyridine and loaded with Palladium). The detection of Si and O is consistent with the silica framework that forms the backbone of the HMSNs, while the presence of C and N can be attributed to the successful attachment of organic functional groups—likely the pyridine (Pyra) moiety—used to functionalize the silica surface. The Pd signal in the spectrum confirms the incorporation or loading of palladium nanoparticles within or onto the silica matrix.

The appearance of these elemental peaks in the EDX spectrum provides strong evidence of successful surface modification and metal loading, supporting the intended synthesis strategy. Moreover, the distribution and relative intensity of the peaks can be used qualitatively to estimate the elemental distribution and to verify that no significant contaminants are present in the final product. These results are in line with previous studies where EDX has been effectively used to confirm surface functionalization and metal doping in nanostructured materials (Wang *et al*., 2015; He *et al*., 2020).

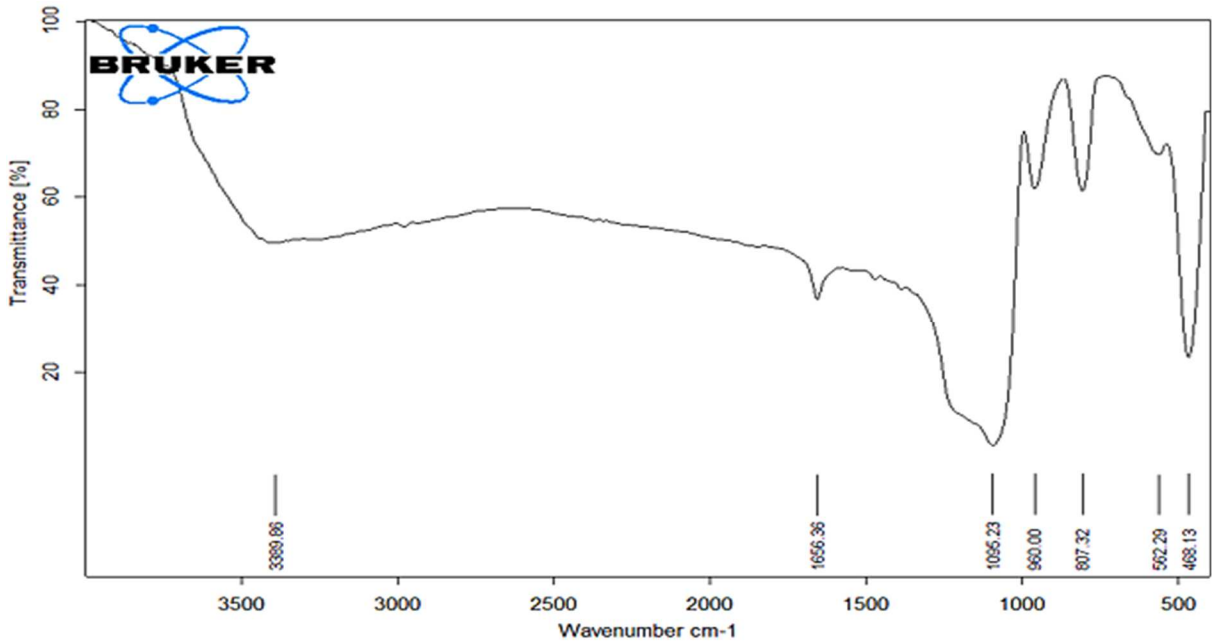

Fig 1. FT-IR spectrum of HMSNs~Pyra/Pd nanoparticles.

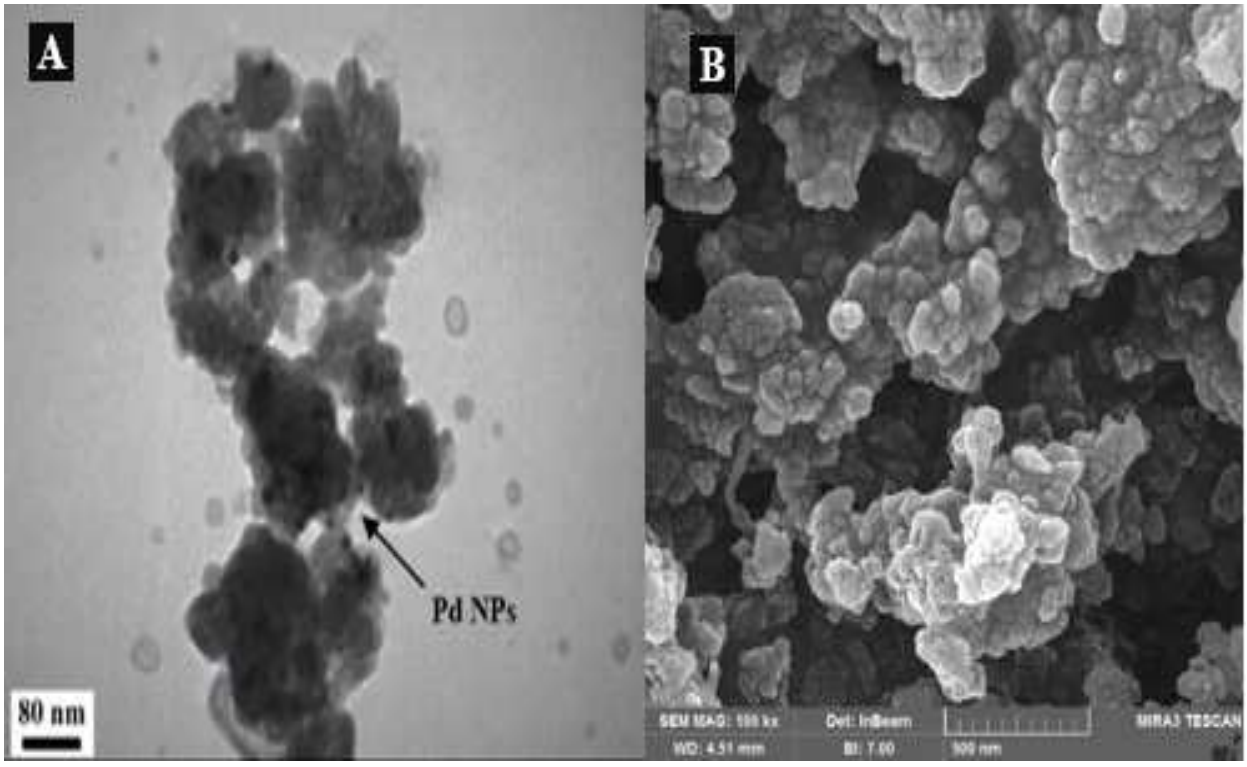

Fig 2. **A) TEM image**; **B) SEM image** of **HMSNs~Pyra/Pd nanoparticles**.

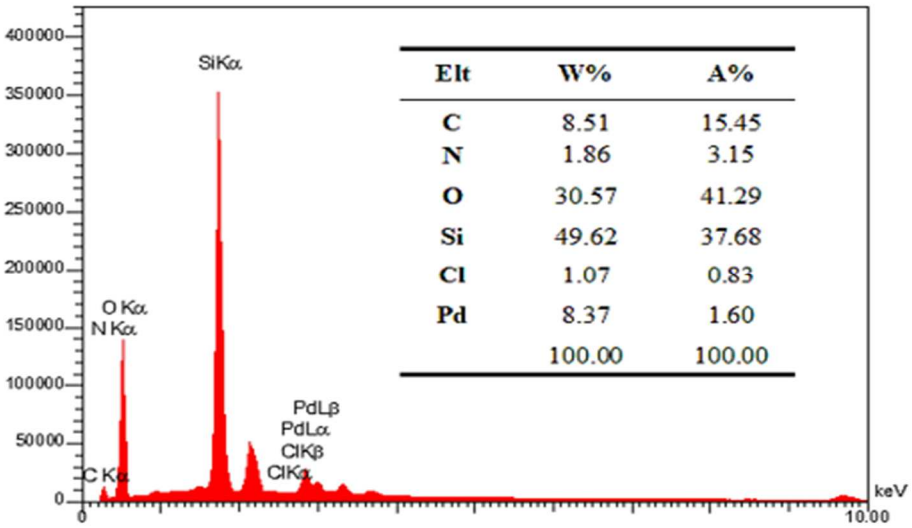

Elt	W%	A%
C	8.51	15.45
N	1.86	3.15
O	30.57	41.29
Si	49.62	37.68
Cl	1.07	0.83
Pd	8.37	1.60
	100.00	100.00

Fig 3. EDX spectrum of HMSNs~Pyra/Pd nanoparticles. Element= Elt, Weight [%] = W% and Atom [%] = A%

Effect of palladium nanoparticles on germination traits of Camelina: The results of the analysis of variance (Table 1) at the germination stage of the Camelina plant showed that there was a highly significant difference at the 1% statistical level among all studied traits, including germination percentage, root length, shoot length, Seedling length and the root-to-shoot ratio. The mean comparison for the studied traits was conducted using Duncan's test at the 5% statistical level, as shown in Fig 4. As shown in Fig 4a, the highest germination percentage was observed in the control group (95%), while the lowest percentage (11.67%) was recorded at the concentration of 200 mg/L palladium nanoparticles. For root length (Fig 4b), the maximum value (1.87 cm) was found in the control group, whereas the minimum value (0.23 cm) was observed at 200 mg/L PdNPs. Similarly, for shoot length (Fig 4c), the highest value (2.61 cm) was recorded in the control, while the lowest value (0.3 cm) was associated with 200 mg/L PdNPs. Regarding seedling length (Fig 4d), the control group exhibited the longest seedling length (4.49 cm), whereas the shortest seedling length (0.4 cm) was observed at 200 mg/L PdNPs. Moreover, the highest root-to-shoot length ratio (0.77 cm) (Fig 4e) was found at 200 mg/L PdNPs, while the lowest ratio (0.48 cm) was recorded at 50 mg/L PdNPs. Additionally, Fig 5 illustrates the effect of different concentrations of palladium nanoparticles on Camelina seed germination (Szőllősi *et al*., 2020).

Table 1. Analysis of Variance of germination traits in Camelina

		Mean of Square				
S.O.V	df	Germination percentage	Root length	Shoot length	Root length/Shoot length	Seedling length
Pd NPs	3	12300.000**	5.576**	10.033**	0.162**	31.565**
Error	8	166.667	0.009	0.013	0.025	0.097
Total	12					

**, significance at the 1% level.

The results of the correlation analysis among the studied traits (Figure 6) revealed strong and highly significant positive relationships between key germination and seedling growth parameters. Notably, germination percentage exhibited a very strong positive correlation with shoot length ($r = 0.949^{**}$), root (radicle) length ($r = 0.909^{**}$), and total seedling length ($r = 0.939^{**}$). These correlations indicate that higher germination rates are closely associated with more vigorous and elongated seedling growth. This finding suggests that the physiological and environmental factors that enhance germination—such as hormonal regulation, water uptake efficiency, and energy mobilization—also contribute significantly to post-germination growth and early seedling vigor (Supriya *et al*., 2024; Bewley *et al*., 2013). Furthermore, seedling length was almost perfectly correlated with shoot length ($r = 0.999^{**}$) and root length ($r = 0.996^{**}$), reflecting a tightly coordinated pattern of above- and below-ground development. Such high

correlation values imply that increases in seedling length are proportionally distributed between shoot and root systems. This integrated development is essential during early seedling establishment, as both shoot elongation (for light capture and photosynthesis) and root extension (for anchorage and water/nutrient uptake) are critical to plant survival and subsequent growth stages (Pasternak *et al*., 2023). Additionally, the correlation between root length and shoot length ($r = 0.993^{**}$) was also highly significant and positive, highlighting a synchronized developmental trajectory of these two major plant axes. This strong relationship likely results from shared physiological processes such as meristematic activity, hormone signaling (e.g., auxins and cytokinins), and the allocation of assimilates during early development (Zhang *et al*., 2016). A robust root system facilitates efficient water and mineral nutrient uptake, which in turn supports shoot growth and leaf expansion. Conversely, healthy shoot development enhances the plant's photosynthetic capacity, providing energy and organic compounds that stimulate root proliferation.

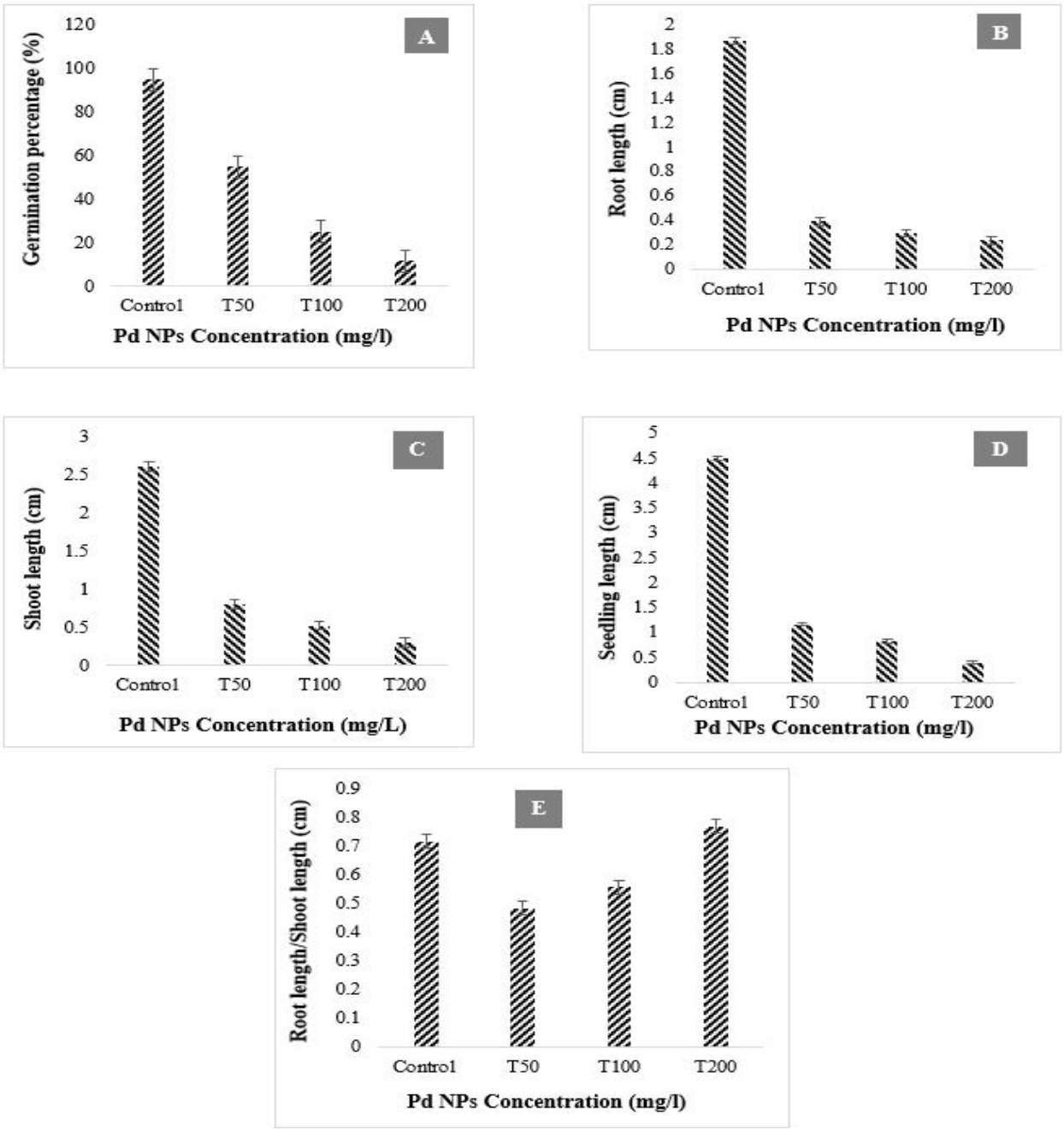

Figure 4. Mean comparision of traits in germination test.

Fig 5. **The effect of different concentrations of palladium nanoparticles on seed germination of Camelina plant**

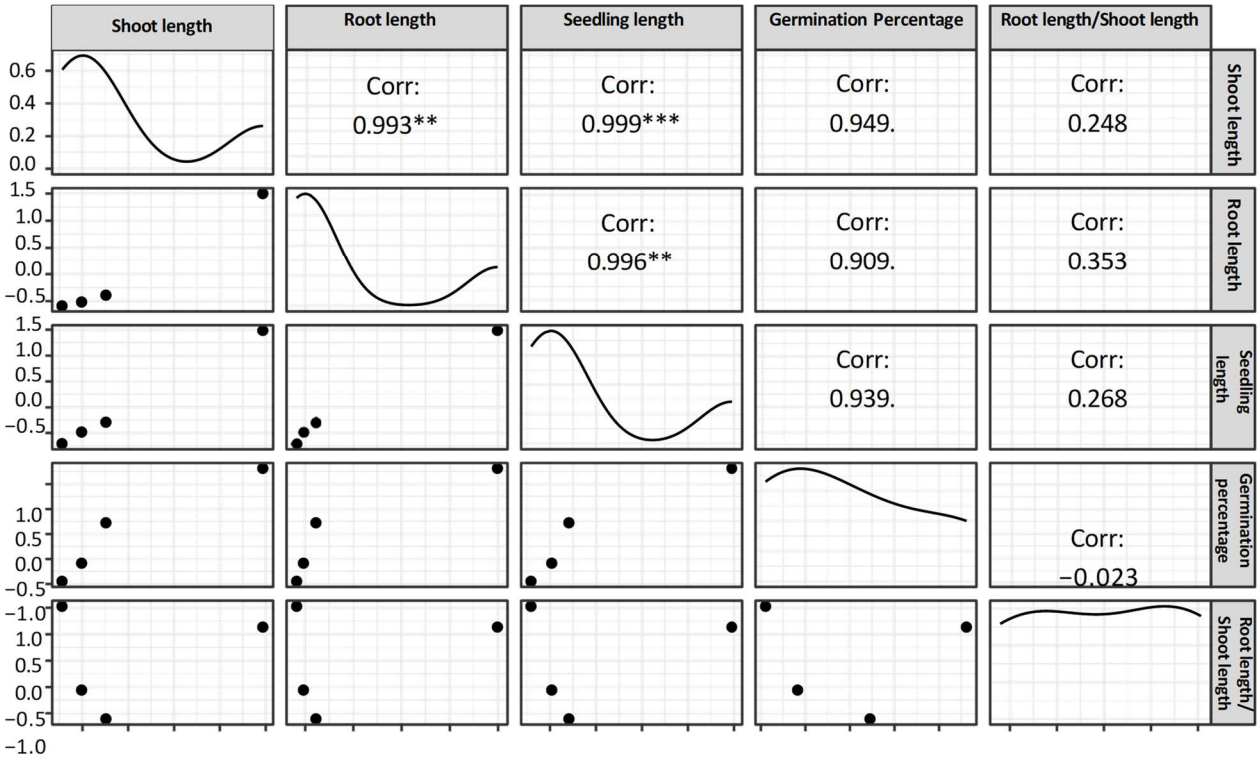

Fig 6. Correlation analysis of the studied traits in the germination test.

The results of the heatmap analysis (Fig. 7) revealed a clear separation of the studied treatments into two distinct clusters based on their impact on seedling growth traits. The first group, consisting solely of the control treatment (0 mg/L palladium nanoparticles), was associated with the highest recorded values for key germination and growth parameters, including seedling length, radicle length, shoot length, and germination percentage. This outcome suggests that under nanoparticle-free conditions, Camelina seeds were able to germinate and grow under optimal physiological conditions, likely due to the absence of nanoparticle-induced stress factors. Normal cellular metabolism, hormonal balance, and unimpeded nutrient and water absorption could have contributed to this enhanced performance (Tripathi *et al*., 2017). In contrast, the second group—which comprised treatments with increasing concentrations of PdNPs (50, 100, and 200 mg/L)—displayed a distinct pattern characterized by reduced seedling vigor. Specifically, these treatments were associated with significantly lower values for all growth indices, including radicle and shoot length, except

for the radicle-to-shoot length ratio, which was elevated. The increased radicle-to-shoot ratio may reflect a stress-adaptive response, in which energy and resources are diverted to radicle growth in an attempt to optimize water uptake under nanoparticle-induced stress conditions (Kumari *et al*., 2024). However, this morphological adjustment comes at the cost of overall seedling development and health. The observed inhibitory effects of PdNPs may be attributed to several underlying mechanisms. One prominent hypothesis involves oxidative stress triggered by an overproduction of reactive oxygen species (ROS), which is a common response to heavy metal and nanoparticle exposure. Excess ROS can cause lipid peroxidation, protein oxidation, DNA damage, and disruption of enzymatic activities, all of which impair normal cellular functioning (Guo *et al*., 2022). Additionally, nanoparticles can physically obstruct water and nutrient uptake by forming aggregates around root surfaces or penetrating plant tissues, thereby altering membrane permeability and ionic balance (Vijay *et al*., 2025). This interference can result in osmotic stress, membrane damage, and disturbed hormonal signaling pathways, especially those involving abscisic acid and auxins, which are essential for germination and early growth.

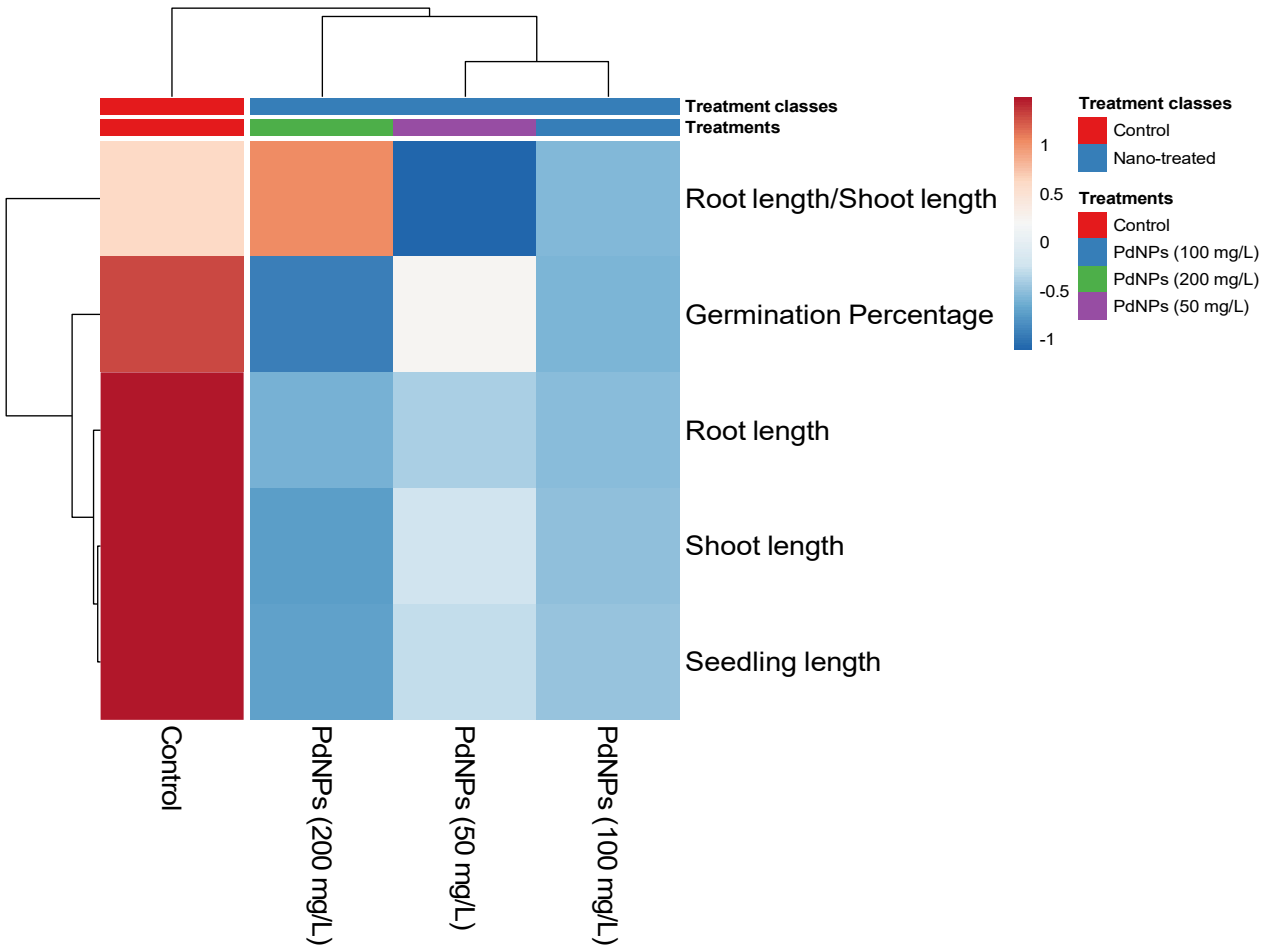

Fig 7. Heatmap Analysis **for the Studied Traits (Both rows and columns are clustered using maximum distance and average linkage).**

Conclusion: In summary, this study successfully synthesized hollow silica nanoparticles loaded with palladium metal (HMSNs~Pyra/Pd) and characterized them using various techniques, including FTIR, TEM, SEM, and EDX. The synthesized nanoparticles had an average size of 30–50 nm, with palladium nanoparticles approximately 5–8 nm in size. Experimental results revealed that different concentrations of palladium nanoparticles had a significant negative impact on the germination traits of *Camelina sativa*, reducing germination percentage, root length, shoot length, and root-to-shoot ratio. The highest germination percentage (95%) was observed in the control group, while the lowest (67.11%) was recorded at the 200 mg/L concentration of palladium nanoparticles. These findings underscore the potential environmental risks associated

with palladium nanoparticles. It is recommended to conduct comprehensive toxicity assessments to evaluate the potential effects of palladium on non-target organisms, soil health, and the broader ecosystem. These investigations should encompass both acute and chronic exposure scenarios to ensure a thorough evaluation of the environmental safety associated with palladium nanoparticles. Additionally, research should focus on elucidating the specific mechanisms underlying the uptake of palladium nanoparticles by plant cells. Employing techniques such as microscopy and molecular labeling can facilitate the tracking of nanoparticle movement within plant tissues and help identify the pathways involved in hormone release and signaling processes. Furthermore, it is essential to assess the long-term impacts of nanoparticle application on plant physiology, yield, and nutritional quality. This assessment should include monitoring plant growth parameters, analyzing nutrient absorption, and evaluating the quality of harvested crops across multiple generations.

Acknowledgements: The authors would like to kindly acknowledge all the support and funding from Razi University.

Funding: This research has been financially supported by Razi University.

Author contribution: Conceptualization, data curation, investigation, and methodology; writing-original draft performed by M Gh. Formal analysis, investigation, and visualization methodology; writing review performed by Z Ch. D K supervised and conceptualized the study, resources, and funding acquisition. All authors interpreted the data and approved the final version.

Declaration of competing interest: The authors declare that they have no conflict of interest.

Data Availability: The datasets used and analysed during the current study are available from the corresponding author on reasonable request.

REFERENCES

Abd-elhamed, R. S (2017). Cytogenetic variability analysis for Allium cepa L in response to green synthesis silver nanoparticles. IJARBS. 4, 73-80. https://doi.org/10.22192/ijarbs.2017.04.05.008

Bewley, J. D., K, Bradford., H, Hilhorst and H, Nonogaki (2013). Seeds: Physiology of Development, Germination and Dormancy (3rd ed.). Springer. https://doi.org/10.1007/978-1-4614-4693-4

Findik, F (2021). Nanomaterials and their applications. Period. Eng. Nat. Sci. 9(3), 62-75. https://doi.org/10.21533/pen.v9.i3.828

Ghorbani, M., D. Kahrizi and Z. Chaghakaboodi (2020). Evaluation of Camelina sativa doubled haploid lines for the response to water-deficit stress. JMPB. 9(2), 193-199. https://doi.org/10.22092/JMPB.2020.351330.1240.

Ghorbani, S., R. Parnian and E. Soleimani (2021). Pd nanoparticles supported on pyrazolone-functionalized hollow mesoporous silica as an excellent heterogeneous nanocatalyst for the selective oxidation of benzyl alcohol. J. Organomet. Chem. 952, 122025. https://doi.org/10.1016/j.jorganchem.2021.122025.

Ghorbani, M., S. Ghorbani., D. Kahrizi and E. Arkan (2025). Development and Characterization of Indole-3-Butyric Acid-Functionalized Fe3O4@ SiO2 Nanoparticles for Improved Plant Root Development. BNSc. 15(3), 329. https://doi.org/10.1007/s12668-025-01949-9.

Ghorbani, M., D. Kahrizi., E. Arkan., F. Aghaz., A. Zebarjadi and S. Ghorbani (2024). Synthesis and characterization of indole-3-butyric acid-loaded hollow mesoporous silica nanoparticles: effects on plant rooting induction. J. Plant Growth Regul. 43, 4506–4516. https://doi.org/10.1007/s00344-024-11411-x.

Golami, A., H. Abbaspour., M. Gerami and H. Hashemi-Moghaddam (2020). Investigation of the effect of titanium dioxide nanoparticles (TiO_2) on photosynthetic pigments and some biochemical and antioxidant properties of Rosmarinus officinalis L. JFST.17(105), 123–134. https://doi.org/10.52547/fsct.17.105.123.

Guo, H., Y. Liu., J. Chen., Y. Zhu and Z. Zhang (2022). The effects of several metal nanoparticles on seed germination and seedling growth: a meta-analysis. Coatings. 12(2), 183. https://doi.org/10.3390/coatings12020183.

Gohar, F., U.Z. Iqbal., M.B. Khan., F. Rehman., F.S.U. Maryam., M. Azmat., S. Munir., H. Iqbal and M.U. Shahid (2024). Impact of Nanoparticles on Plant Growth, Development and Physiological Processes. Compr. Rev. https://doi.org/10.20944/preprints202410.0780.v1.

Heydari, M., S. Shahpesandy., S.M. Mosavi Nik and M. Bijani (2015). Effect of nano-silicon on the germination and seedling growth of landrace and cultivar of wheat (Aestivum sativum). Seed Ecol. 1(1), 1-16. https://doi.org/10.22077/SEJ.2015.366.

He, Q., Z, Zhang., F, Gao., Y, Li, and J, Shi (2020). In vivo biodistribution and urinary excretion of mesoporous silica nanoparticles: Effects of

particle size and PEGylation. Small 7(2), 271–280. https://doi.org/10.1002/smll.201001459.

Karunakaran, G., R. Suriyaprabha., V. Rajendran and N. Kannan (2016). Influence of ZrO_2, SiO_2, Al_2O_3 and TiO_2 nanoparticles on maize seed germination under different growth conditions. IET NBT. 10(4), 171–177. https://doi.org/10.1049/iet-nbt.2015.0007.

Kelij, S and M. Kazemian Ruhi (2018). Sesame seed germination and anatomical changes influenced to silver nanoparticles. J. Plant Res. 30(4), 899-909. https://dor.isc.ac/dor/20.1001.1.23832592.1396.30.4.16.1.

Khan, I., S.A. Awan., M.Rizwan., Z.U.I. Hassan., M.A. Akram., R. Tariq., M. Brestic and W. Xie (2022). Nanoparticle's uptake and translocation mechanisms in plants via seed priming, foliar treatment, and root exposure: a review. Environ. Sci. Pollut. Res. 29, 89823–89833. https://doi.org/10.1007/s11356-022-23945-2.

Kumari, A., A.K. Gupta., S. Sharma., V.S. Jadon., V. Sharma., S.C. Chun and I. Sivanesan (2024). Nanoparticles as a tool for alleviating plant stress: mechanisms, implications, and challenges. Plants, 13(11),1528. https://doi.org/10.3390/plants13111528.

Larsen, S. U and C. Andreasen (2004). Light and heavy turfgrass seeds differ in germination percentage and mean germination thermal time. Crop Science. 44(5), 1710-1720. https://doi.org/10.2135/cropsci2004.1710.

Metsalu, T and J, Vilo (2015). ClustVis: a web tool for visualizing clustering of multivariate data using Principal Component Analysis and heatmap. NAR 43(W1), W566-W570. https://doi.org/10.1093/nar/gkv468.

Prasad, T. N. V. K. V., S. Adam., P. V. Rao., B. R. Reddy and T. G. Krishna (2016). Size dependent effects of antifungal phytogenic silver nanoparticles on germination, growth and biochemical parameters of rice (Oryza sativa L), maize (Zea mays L) and peanut (Arachis hypogaea L). IET NBT. 11(3), 277–285. https://doi.org/10.1049/iet-nbt.2015.0122.

Patidar, P., P. Kumar., S.S. Parmar and N. Khan (2024). Influence of Silver Nanoparticles on Onion (Allium Cepa L.) Seed Germination and Seedling Vigor. J. adv. biol. Biotechnol. 27(8), pp.10-16. https://doi.org/10.9734/jabb/2024/v27i81116.

Pasternak, T., S. Kircher., K. Palme and J.M. Pérez-Pérez (2023). Regulation of early seedling establishment and root development in Arabidopsis thaliana by light and carbohydrates. Planta, 258(4), 76. https://doi.org/10.1007/s00425-023-04226-9.

Sayedena, V., B. Pilehvar., K. Abrari-Vajari., M. Zarafshar and H.R. Eisvand (2019). Effects of TiO2 nanoparticles on germination and primary growth of mountain ash (Sorbus luristanica). IJSR. 6(1), 173-184. https://doi.org/10.29252/yujs.6.1.173.

Supriya, K., U. Bharti., D. Basandrai., S. Bhatia., Y. Vikal., P. Chhuneja and A.K. Basandrai (2024). Relationship between seed traits and seedling parameters in rice wild species. Genet. Resour. Crop Evol. 71(1), 299-308. https://doi.org/10.1007/s10722-023-01623-7.

Szőllősi, R., A. Molnár., S. Kondak and Z. Kolbert (2020). Dual effect of nanomaterials on germination and seedling growth: Stimulation vs. phytotoxicity. Plants. 9(12), 1745. https://doi.org/10.3390/plants9121745.

Soleimani, E., S. Ghorbani., M. Taran and A. Sarvary (2012). Synthesis of 4, 4′-(arylmethylene) bis (3-methyl-1H-pyrazol-5-ol) derivatives in water. C. R. Chim. 15(11-12), 955-961. https://doi.org/10.1016/j.crci.2012.07.003.

Skiba, E., M. Pietrzak., S. Michlewska., J. Gruszka., J. Malejko., B. Godlewska-Żyłkiewicz and W.M. Wolf (2024). Photosynthesis governed by nanoparticulate titanium dioxide. The Pisum sativum L. case study. Environ. Pollut. 340, 122735. https://doi.org/10.1016/j.envpol.2023.122735.

Tripathi, D.K., S. Singh., S. Singh., P.K. Srivastava., V.P. Singh., S. Singh., S.M. Prasad., P.K. Singh., N.K. Dubey., A.C. Pandey and D.K. Chauhan (2017). Nitric oxide alleviates silver nanoparticles (AgNps)-induced phytotoxicity in Pisum sativum seedlings. Plant Physiol Biochem. 110,167-177. https://doi.org/10.1016/j.plaphy.2016.06.015.

Vijay, P. P., S. Kunta and B.A. Venkatesh (2025). Mobility of Nanoparticles in Plants. In Plant-Based Nanoparticle Synthesis for Sustainable Agriculture (pp. 125-139). CRC Press. https://doi.org/10.1201/9781003477730-9.

Wang, Y., Q, Zhao., N, Han., L, Bai., J, Li., J, Liu and S, Wang (2015). Mesoporous silica nanoparticles in drug delivery and biomedical applications. Nanomedicine: NBM or Nanomed-Nanosci. 11(2), 313–327. https://doi.org/10.1016/j.nano.2014.09.014.

Zhang, H., B. G, Forde (2016). An Arabidopsis MADS box gene that controls nutrient-induced changes in root architecture. Science. 279(5349), 407–409. https://doi.org/10.1126/science.279.5349.407.